Cent. Eur. J. Phys. • 9(6) • 2011 • 1440-1445
DOI: 10.2478/s11534-011-0061-0

VERSITA

Central European Journal of **Physics**

# Roughness and fractality of fracture surfaces as indicators of mechanical quantities of porous solids

**Research Article**

Tomáš Ficker[1]*, Dalibor Martišek[2]

1 *Brno University of Technology, Faculty of Civil Engineering, Department of Physics, Veveří 95, 602 00 Brno, Czech Republic*

2 *Brno University of Technology, Faculty of Mechanical Engineering, Department of Mathematics, Technická 2, 616 62 Brno, Czech Republic*

**Received 10 November 2010; accepted 10 June 2011**

**Abstract:** The 3D profile surface parameter $H_q$ and fractal dimension $D$ were tested as indicators of mechanical properties inferred from fracture surfaces of porous solids. High porous hydrated cement pastes were used as prototypes of porous materials. Both the profile parameter $H_q$ and the fractal dimension $D$ showed capability to assess compressive strength from the fracture surfaces of hydrated pastes. From a practical point of view the 3D profile parameter $H_q$ seems to be more convenient as an indicator of mechanical properties, as its values suffer much less from statistical scatter than those of fractal dimensions.

**Keywords:** roughness analysis • fracture surfaces • cement-based materials • confocal microscopy • fractals



## 1. Introduction

Fracture surfaces of solids bear information not only on the fracture process itself but also on various mechanical quantities. In order to read the surface information, it is necessary to find a convenient tool capable of decoding the surface message.

The present paper is aimed at two parameters that might become useful in the decoding procedure. One of those parameters is the three-dimensional (3D) surface profile parameter $H_q$, which quantifies the height irregularities of surfaces. It is a global parameter representing the average height of the 3D surface profile. The second investigated parameter is the fractal dimension of the 3D profile. This dimension $D$ characterizes "compactness" of the 3D surface profile rather than its corrugation which is a domain of the $H_q$ parameter. The goal of this study is to verify the capability of these two parameters to evaluate mechanical data, such as those of compressive strength, from the morphological arrangements of the fracture surfaces of porous solids. In addition, the results achieved in this study enable us to make some conclusions about the effectiveness of both the parameters. The hydrated cement paste has been chosen as a prototype of porous solids since its various values of porosity can easily be set by the original water-to-cement ratio.

In the research field of cementitious materials there are only a restricted number of studies that deal with the surface features of fractured specimens. Some of the early surface studies of hydrated cement materials were focused

*E-mail: ficker.t@fce.vutbr.cz

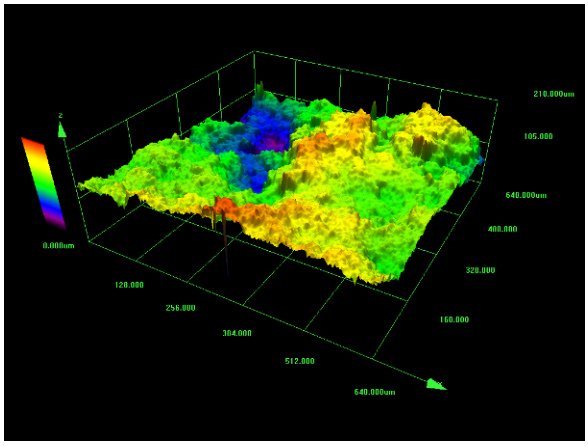


**Figure 1.** Confocal reconstruction of the surface relief of the fracture sample made of hydrated cement paste.

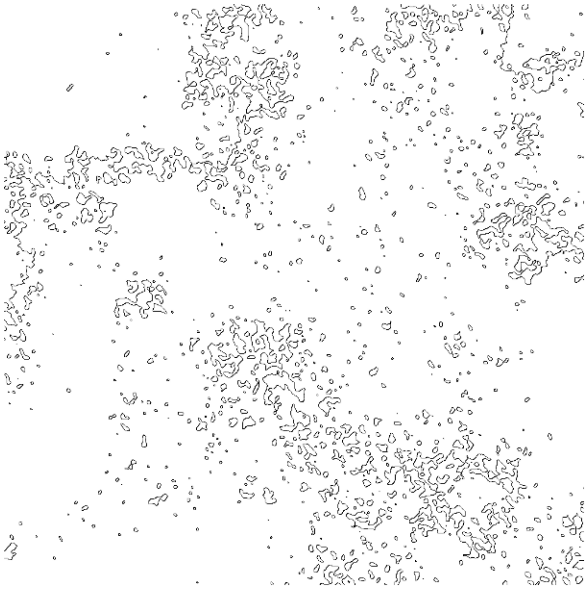

**Figure 2.** One of the horizontal sections of the surface relief showing the set of isolines.

on fractal properties [1, 2] whereas others [3–5] investigated roughness numbers ($RN$) or similar surface characteristics [6–8]. The related study of the surface roughness and strength of cement pastes has been published only recently [9], but it has not included any results concerning fractal dimensions and their connections with the compressive strength of the material. However, it has indicated a relation between profile parameters and compressive strength. This also inspired our intention to perform a comparative study concerning the 3D profile parameter $H_q$ and fractal dimension $D$ as possible indicators of mechanical quantities of porous solids.

## 2. Fractal dimension $D$ and surface profile parameter $H_q$

***The fractal dimensions*** $D$ of fracture surfaces were computed by means of surface reliefs created by the confocal microscope in the form of digital matrices $[x_i, y_i, z_i]$. From these digital three-dimensional reliefs (see Fig. 1) a series of horizontal sections were extracted and saved into bitmap files, where each such file represented horizontal isolines (contour lines — see Fig. 2). Every bitmap file was processed with the computer program MULTIFRAN to determine the dimension $D_0$ of the corresponding section. All the dimensions $D_0$ belonging to the particular relief were averaged $\overline{D_0}$ and the resulted dimension $D$ of the relief was calculated as $D = 1 + \overline{D_0}$.

The software MULTIFRAN is actually based on the multifractal formalism and was developed in our laboratory to conduct image analyses of the Lichtenberg figures; however, the software is also convenient for processing the bitmap images of isolines. In the next paragraphs the multifractal formalism is briefly described.

Let us suppose that the investigated fractal object is embedded in the Euclidean space of the topological dimension $E$. This space is partitioned into an $E$-dimensional grid whose basic cell is of a linear size $\varepsilon$ (arrangement necessary for the *box-counting method*). One of the topological partition sums used in this field is defined by the probability moments

$$m_q(\varepsilon, q) = \sum_{i=1}^{I} p_q^i(\varepsilon), \quad p_i(\varepsilon) = \left(\frac{n_i}{N}\right), \tag{1}$$

$$\sum_{i=1}^{I} p_i(\varepsilon) = 1, \quad q \in (-\infty, +\infty),$$

where the symbol $n_i$ represents the number of points in the $i$-th cell and $N$ is the number of all points of the fractal object studied.

The goal of the multifractal analysis is to determine one of the three multifractal spectra. The most frequently used spectrum is that of generalized dimensions $D_q$

$$D_q = \lim_{q^* \to q} \frac{\partial \ln m(\varepsilon, q)}{(q^* - 1)\, \partial \ln \varepsilon}. \tag{2}$$

As has been mentioned, the investigated fractal objects are in the form of graphical bitmap files. Their plane of graphical pixels (points) is covered with a two-dimensional

grid whose basic cell is of the linear size $\varepsilon$ pixels. Using this grid the partition sum (1) is computed. Since the covering of the plane with a grid is arbitrary and the position of the grid should not influence the results, we used several positions of the grid to find the average value of the partition sum $M_q(\varepsilon,q)$. For each $\varepsilon$-grid there are $\varepsilon^2$ independent coverings generated by shifting the grid origin within the first $\varepsilon$-cell

$$M_q(\varepsilon) = \frac{1}{\varepsilon^2}\sum_{j=1}^{\varepsilon^2} m_j(\varepsilon,q)\,. \tag{3}$$

Such a procedure requires the fractal set to be embedded in a larger grid that allows one to move the origin without the loss of any part of the fractal object. The averages $M_q(\varepsilon)$ are estimated for a series of $\varepsilon$-grids and the slopes in the bilogarithmic plot $(\ln\varepsilon, \ln M_q(\varepsilon))$ are calculated using the linear regression method. These slopes divided by the corresponding $(q-1)$ values represent the generalized dimensions $D_q$. Different $D_q$ values for an analyzed object indicate *multifractal* behavior while identical values signify *monofractal* behavior. Our investigated images showed a degenerate $D_q$ spectrum, i.e. monofractal behavior with a single value of dimension $D_0$. The complete computer[1] processing of one surface relief lasted approximately one hour. In this study 540 reliefs were analyzed.

**The surface profile parameters** $H_q$ were also derived from the 3D digital surface reliefs created by the confocal microscope. The fracture reliefs were modeled by a function $z=f(x,y)$ from which the $H_q$ parameter was calculated as follows

$$H_q = \sqrt{\frac{1}{L\cdot M}\iint_{(LM)}[f(x,y)]^2\,dx\,dy}, \tag{4}$$

where $L\times M$ is the area of the vertical projection of the surface function $f(x,y)$ into the horizontal plane $xy$.

## 3. Experimental arrangement

108 specimens (2 cm × 2 cm × 16 cm) of hydrated ordinary Portland cement paste of six water-to-cement ratios $r$ (0.3, 0.4, 0.5, 0.6, 0.7, 0.8) were prepared (eighteen samples per $r$-value). The specimens were rotated during hydration to achieve better homogeneity. All specimens were stored throughout hydration at 100% RH and 20°C. After 60 days of hydration the specimens were fractured in a three-point bending arrangement and the fracture surfaces were immediately used for microscopic analysis. Other parts of the specimens were used for porosity measurements and compressive tests.

Since each group of specimens of the particular water-to-cement ratio $r$ consisted of eighteen specimens, the same number of small cubes with an edge of 2 cm were subjected to compressive tests. Therefore, each point on the graph $\sigma_c(P)$ represents an average of eighteen compressive tests. The surfaces of the cubes were perfectly processed to remove corrugations and to create a good interface between the specimens and the plates of the hydraulic press. The gradually increasing compressive stress in the static region acted on the cubes up to their breakdown.

Porosity was determined by the common weight-volume method. The wet specimens were weighted, their volume measured, then subjected to 105°C for one week until their weight did not change and the dry specimens were weighted again.

The microscopic analysis was performed by using an Olympus Lext 3100 confocal microscope. Approximately 150 image sections were taken for each measured surface site starting from the very bottom of the surface depressions (valleys) to the very top of the surface protrusions (peaks). The investigated area $L\times M = 1280\ \mu\text{m}\times 1280\ \mu\text{m}$ (1024 pixels × 1024 pixels) was chosen in five different places of each fracture surface (in the center and in the four positions near the corners of the rectangular area), i.e. each plotted point of the graph of the profile parameter $H_q$ corresponds to an average value composed of 90 measurements (18 samples×5 surface measurements). The digitalized fracture surfaces were subjected to 3D profile surface analyses to compute $H_q$ values using the software Olympus Lext 3100, version 6. The fractal dimensions were calculated from the digitalized surfaces by means of the software MULTIFRAN described in Section 2.

## 4. Results and discussion

It is well known that porosity is one of the main factors determining compressive strength of cement-based materials. Particularly with hydrated cement pastes, porosity becomes a decisive factor governing the mechanical strength. Although there are more functional relationships between compressive strength $\sigma_c$ and porosity $P$, the Balshin relation [10]

$$\sigma_c = \sigma_0(1-P)^k\,,\quad \sigma_0,\ k \text{ material constants.} \tag{5}$$

[1] *PC: AMD Turion 64x2 MT TL-62, 2.10 GHz, 4 GB RAM.*

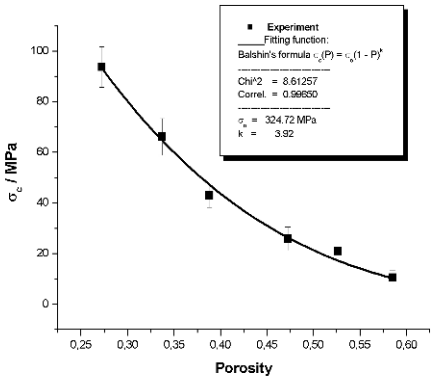


**Figure 3.** Compressive strength as dependent on the porosity of hydrated Portland cement paste.

seems to be quite fundamental. Compared with the classical Powers relation [11]

$$\sigma_c = \sigma_0 \cdot \chi^3, \ \chi \text{ gel}-\text{space ratio.} \tag{6}$$

the Balshin relation looks like an equivalent formula to that of Powers since the gel-space ratio $\chi$ may be expressed as $\chi \approx (1 - P)$. However, due to the general fitting parameter $k$, the Balshin formula might be considered a bit more general. It is interesting to note that both the relations were presented nearly simultaneously although for different materials. The Balshin formula has been used as a fitting pattern and applied to our data. Fig. 3 shows the result of the fitting procedure. A typical convex shape of the dependence $\sigma_c(P)$ can be seen with a very high correlation coefficient reaching almost one. This confirms a mutual consistency between the used fitting pattern and the measured data.

The illustrated high correlation between compressive strength and porosity guarantees that every other quantity dependent on porosity will similarly correlate to the value of compressive strength. This issue was also tested in the recently published communication [9]. In that preliminary communication the 3D profile and roughness parameters were chosen as testing objects and their dependence on porosity as well as their correlation to compressive strength were clearly indicated. The profile parameters evaluated within 20x magnification were proved to be the most reliable from a statistical viewpoint. The present study is focused on the profile parameter $H_q$, which is one of the most reliable parameters tested previously. This parameter is subjected to a more detailed investigation based on both the larger set of specimens and the direct measurement of porosity (the porosity measurements being omitted in the preliminary communication [9]). Fig. 4 shows both the dependences $H_q(P)$ and $\sigma_c(H_q)$. Since there is no theory determining convenient fitting patterns for those dependences, intuitive curves (dashed lines) were inserted in both the plots. It can be seen that there are quite small statistical scatters of measured points along the curves.

As expected, the dependence $H_q(P)$ in Fig. 4 represents a monotonically increasing function since higher porosity causes rougher fracture surfaces with larger protrusions (peaks) and deeper depressions (valleys) in the surface relief. On the other hand the dependence $\sigma_c(H_q)$ shows a monotonically decreasing function, which is understandable when bearing in mind the behavior of $\sigma_c(P)$ and $H_q(P)$ — larger $H_q$ means larger $P$ which ensures smaller $\sigma_c$. In other words, the rougher fracture surfaces of porous solids inform us of the smaller mechanical strength of these materials. It is interesting to notice the striking similarity between the graphs of $\sigma_c(P)$ and $\sigma_c(H_q)$ in Fig. 3 and Fig. 4 respectively, which might evoke the idea of their related generic origins.

As can be seen in Fig. 5, the fractal dimensions $D$ of fracture surfaces also manifest a dependence on porosity. However, the graph of $D(P)$ does not show increasing tendency as in the case of $H_q(P)$ but, on the contrary, a decrease. The differing behavior of $H_q(P)$ and $D(P)$ is understandable when their different origins are taken into account. For example, the fracture surfaces of high porous materials are described by a high value of $H_q$ since this parameter quantifies height irregularities of surfaces, but the corresponding value of fractal dimension $D$ is small because $D$ quantifies "compactness" of the surface relief rather than its height irregularity. High porous solids generate the fracture reliefs of essential height irregularity but of low "compactness", and for this reason the surfaces of their fragments manifest higher values of profile parameters and lower values of fractal dimensions.

Since fractal dimension is dependent on porosity, it is expected that it will be correlated to compressive strength as well. This is documented at the right hand side of Fig. 5 where the dependence $\sigma_c(D)$ is graphically plotted. The graph of $\sigma_c(D)$ shows an increasing tendency which can be derived from the behavior of $D(P)$ and $\sigma_c(P)$. A larger statistical scatter of the experimental points within the graph $\sigma_c(D)$ is obvious and is comparable with the statistical scatter visible within the $D(P)$ graph.

Comparing $H_q(P)$ versus $D(P)$ as well as $\sigma_c(H_q)$ versus $\sigma_c(D)$, one striking difference cannot be omitted, namely the larger statistical scatter of points within the graphs $D(P)$ and $\sigma_c(D)$ as compared with $H_q(P)$ and $\sigma_c(H_q)$ respectively. The reason is in the extensive numerical operations necessary for determining fractal dimensions and in the approximate nature of the box-counting method it-

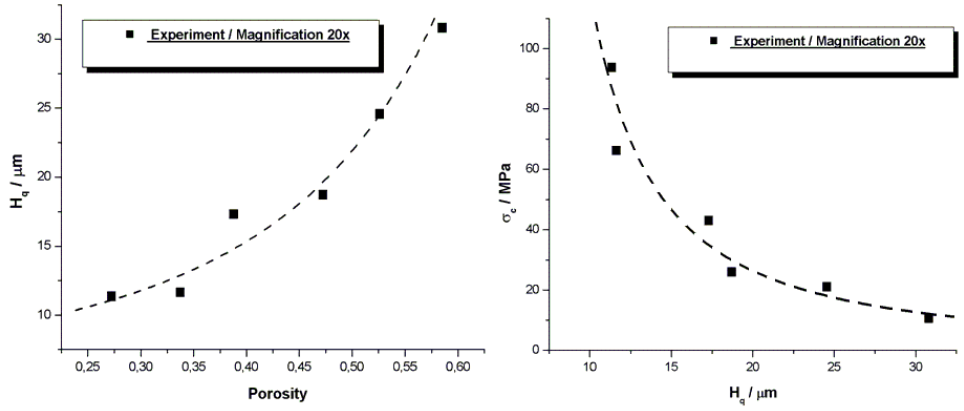


**Figure 4.** The dependence of the 3D profile parameter $H_q$ on porosity (left hand side) and the dependence of compressive strength on the parameter $H_q$ (right hand side).

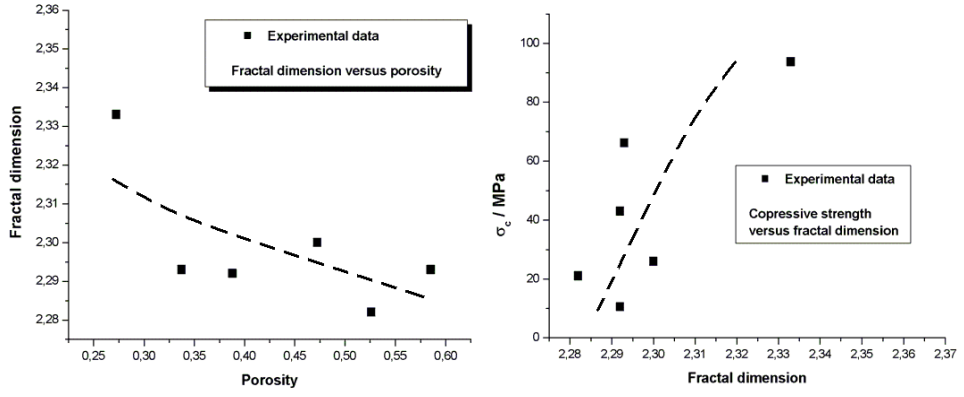


**Figure 5.** The dependence of fractal dimension $D$ on porosity (left hand side) and the dependence of compressive strength on fractal dimension (right hand side).

self. In addition, the method of relief isolines also adds some statistical uncertainty. From a practical point of view, the assessment of compressive strength on the basis of the 3D profile parameter $H_q$ would surely be easier and more reliable. The striking similarity of the graphs $\sigma_c(P)$ and $\sigma_c(H_q)$ also supports this conclusion. Moreover, the determination of 3D profile parameters is numerically less complicated and does not require as much computer time as in the case of fractal dimensions. This does not mean that all fractal dimensions are conceptually unreliable for indicating mechanical properties of porous solids, and would probably be more competitive compared to 3D profile parameters if a more precise computational method were available.

## 5. Conclusion

The comparative study focused on the 3D profile parameter $H_q$ and fractal dimension $D$ as indicators of mechanical properties of porous solids, and revealed the main differences in the capabilities of these quantities to infer compressive strength from fracture surfaces. Due to the numerically less reliable computational model presently available for the processing of fractal dimensions of fracture surfaces, they suffer from a larger statistical scatter as compared with the values of the 3D parameter $H_q$. From a practical point of view the profile parameter $H_q$ seems to be more convenient for the assessment of compressive strength. The employment of fractal dimensions for this purpose depends on developing a more precise computational model with reduced statistical uncertainty.

## Acknowledgements

This work was supported by the Ministry of the Czech Republic under Contract no. ME 09046 (Kontakt).

## References

[1] D. A. Lange, H. M. Jennings, S. P. Shah, Ceram. Trans. 16, 347 (1992)
[2] M. A. Issa, A. M. Hammad, Cem. Concr. Res. 23, 7 (1993)
[3] D. A. Lange, H. M. Jennings, S. P. Shah, J. Mater. Sci. 28, 3879 (1993)
[4] D. A. Lange, H. M. Jennings, S. P. Shah, J. Am. Ceram. Soc. 76, 589 (1993)
[5] D. Zampini, H. M. Jennings, S. P. Shah, J. Mater. Sci. 30, 3149 (1995)
[6] D. A. Lange, C. Quyang, S. P. Shah, Adv. Cem. Bas. Mater. 3, 20 (1996)
[7] A. B. Abell, D. A. Lange, Int. J. Solids Struct. 35, 4025 (1997)
[8] A. B. Nichols, D. A. Lange, Cem. Conc. Res. 36, 1098 (2006)
[9] T. Ficker, D. Martišek, H. M. Jennings, Cem. Conr. Res. 40, 947 (2010)
[10] M. Y. Balshin, Dokl. Akad. Nauk SSSR 67, 831 (1949) (in Russian)
[11] T C. Powers, Am. Ceram. Soc. 41, 1 (1958)